

3-23-2016

Assessment of Acrolein-induced Toxicity Using In-vitro Modeling to Evaluate the Role of PARP Inhibitors in Reducing Cytotoxicity

Kristina Marie Harand

Follow this and additional works at: <http://scholarcommons.usf.edu/etd>

 Part of the [Toxicology Commons](#)

Scholar Commons Citation

Harand, Kristina Marie, "Assessment of Acrolein-induced Toxicity Using In-vitro Modeling to Evaluate the Role of PARP Inhibitors in Reducing Cytotoxicity" (2016). *Graduate Theses and Dissertations*.
<http://scholarcommons.usf.edu/etd/6091>

This Thesis is brought to you for free and open access by the Graduate School at Scholar Commons. It has been accepted for inclusion in Graduate Theses and Dissertations by an authorized administrator of Scholar Commons. For more information, please contact scholarcommons@usf.edu.

Assessment of Acrolein-induced Toxicity Using In-vitro Modeling to Evaluate the Role of PARP
Inhibitors in Reducing Cytotoxicity

by

Kristina Marie Harand

A thesis submitted in partial fulfillment
of the requirements for the degree of
Master of Science in Public Health
Department of Environmental and Occupational Health
with a concentration in Toxicology and Risk Assessment
College of Public Health
University of South Florida

Co-Major Professor: Marie Bourgeois, Ph.D.
Co-Major Professor: Giffe Johnson, Ph.D.
Raymond D. Harbison, Ph.D.

Date of Approval:
March 22, 2016

Keywords: H9c2(2-1), Poly(ADP-Ribose) Polymerase, Cytotoxicity, Acrolein

Copyright © 2016, Kristina Marie Harand

ACKNOWLEDGMENTS

I wish to express my gratitude to the thesis committee, Dr. Marie Bourgeois, Dr. Raymond D. Harbison, and Dr. Giffe Johnson, thank you for your patience, guidance, expertise, understanding, and support which added considerably to my graduate experience. I would like to express my sincere gratitude to my program advisor Dr. Marie Bourgeois, I could not have imagined having a better mentor to guide me through my MSPH. I wish to acknowledge the Environmental and Occupational Health Department at the College of Public Health for my acceptance into this program and their continued support. Thank you to the research committee who awarded me the College of Public Health Student Research Scholarship which helped to financially support this thesis. I would like to acknowledge Dr. Jill Roberts, working for you has been a complete blessing and I appreciate all the advice you have shared. I would also like to acknowledge Dr. Hana Osman and Dr. Thomas Bernard for covering my OSHA 40-Hour HAZWOPPER training. Thank you Ellen Kent and the USF Health Service Corps for providing me an avenue to participate in meaningful, rewarding, community service activities which allowed me to remain humble. To all my friends, I cannot express my thanks enough for your encouragement, understanding and humor which carried me through my many crisis moments. To my best friends Sahara Soliman, Jamie Crowell, Lauren Malloy, Frances Falcon, and Alexis Killeen, having your love and support throughout my many awkward life stages has helped fortify me into the woman I am today. Each one of you has given me more than I could ever hope to give back and I am incredibly thankful to know you. Thank you to the many cohorts who became lifelong friends, spending late nights and weekends with you in the computer lab gave me the

encouragement to achieve finishing this thesis. To Brennan Hodge, thank you for being there to lean on in my failures and to celebrate in my successes. Thank you to my family who has always supported my many pursuits, without your love and guidance I would not be who I am today. To my father, you have given me courage, strength and determination my whole life and all I hope for is to make you proud. To my mother, your kindness, compassion and strength has always inspired me to follow in your footsteps. Thank you to my many lab mates including Daniel Mejia, Brittany Piver, Jayme P. Coyle, and Ushang Desai, your guidance and assistance through this process was invaluable. Finally I wish to give an extra special thanks to Jayme C. Coyle for without him I wouldn't have survived. Thank you for providing me guidance, clarification, assistance and humor to endure my eighteen hour lab days. Most importantly thank you for your friendship which has strengthened my faith in humanity. Lastly I would like to dedicate this thesis in loving memory to my grandfather Charles Z. Culpepper, I will always be G-Pa's girl.

TABLE OF CONTENTS

List of Figures	ii
Abstract	iii
Chapter One: Introduction	1
Acrolein.....	1
H9c2 (2-1) Model	3
Poly(ADP-Ribose) Polymerase Activity	4
DIQ- 1,5-dihydroxyisoquinoline	7
Chapter Two: Methods	9
Cell Culture.....	9
Treatment	10
Poly(ADP-Ribose) Polymerase Activity	10
Cytotoxicity Assessment.....	13
MTT, 3-(4,5-Dimethylthiazol-2-Yl)-2,5-Diphenyltetrazolium Bromide	13
AST, Aspartate Aminotransferase	14
Spectrophotometric Quantification.....	14
Statistical Analysis.....	15
Chapter Three: Results.....	16
Summary: Cytotoxicity.....	16
Poly(ADP-Ribose) Polymerase Activity	16
Toxicological Endpoints	19
MTT, 3-(4,5-Dimethylthiazol-2-Yl)-2,5-Diphenyltetrazolium Bromide	19
AST, Aspartate Aminotransferase	21
Chapter Four: Discussion.....	24
Chapter Five: Conclusion	30
References.....	31

LIST OF FIGURES

Figure 1: Poly(ADP-Ribose) Activity 30 Minutes	18
Figure 2: Poly(ADP-Ribose) Activity 55 Minutes	18
Figure 3: Poly(ADP-Ribose) Activity Comparison.....	19
Figure 4: MTT Activity	20
Figure 5: Vehicle Box Plot MTT	21
Figure 6: DIQ Box Plot MTT	21
Figure 7: Aspartate Aminotransferase Activity	22
Figure 8: Vehicle Box Plot AST.....	23
Figure 9: DIQ Box Plot AST	23

ABSTRACT

Acrolein is an electrophilic α , β -unsaturated aldehyde. Additionally, acrolein is a metabolite of the antineoplastic alkylating agent cyclophosphamide and is implicated in off-target effects, including to bladder hemorrhagic cystitis and cyclophosphamide-induced cardiotoxicity, both of which have led to serious secondary iatrogenic injury during and following chemotherapy. At low concentrations acrolein inhibits cell proliferation without inducing apoptosis, while at high concentrations may result in secondary apoptosis promotion. This investigation assessed the role of the enzyme poly (ADP-ribose) polymerase (PARP) in acrolein induced toxicity using the established toxicological H9c2 (2-1) cardiomyoblast in vitro model. H9c2 (2-1) cells were plated in 24-well plates at 75,000 cells per well three days prior to testing, followed by acrolein dosing at concentrations between 10 μ M and 1000 μ M for either 30 or 55 minutes. PARP activity was quantitatively measured in total cell lysates using a biotin-avidin-conjugated horseradish peroxidase-TMB reporter system in a 96-well microplate format. The lowest effective dose of toxicity at 30 minute dosing was found at 25 μ M (PARP Activity 1.65-fold control) which returned to baseline at 100 μ M; concentrations at or above 250 μ M results in significant PARP activity reductions (\leq 0.46-fold control). Biomarkers were further characterized for cytotoxicity (AST presence), and viability (MTT reduction) in order to facilitate mechanistic characterization of PARP-mediated acrolein cardiotoxicity. Investigation of a PARP inhibitor was assessed to explore the intervention for acrolein induced cardiac tissue damage.

CHAPTER ONE:

INTRODUCTION

Acrolein

Acrolein (C₃H₄O, CAS No. 107-02-8) is a α,β -unsaturated aldehyde which is extremely electrophilic. According to the American Cancer Society 1:8 or 12% of women in America will develop breast cancer within their lifetime, excluding skin cancers breast cancer is the most common cancer of women in America (American Cancer Society, 2016). Cyclophosphamide as an antitumor prodrug is commonly used for treatment of broad spectrum human cancers. Routinely, it is most prescribed for treatment of breast cancers, ovarian cancers and lymphomas (Chan, 1984). Cyclophosphamide is itself inactive, thus requiring an enzyme mediated bioactivation to induce cytostatic activity. As a prodrug cyclophosphamide is categorized as an alkylating agent, once it undergoes activation it forms aldophosphamide. The active metabolite of cyclophosphamide is phosphoramidate mustard and the toxic metabolite is acrolein both are produced during biotransformation of aldophosphamide (Conklin et al., 2015). Phosphoramidate mustard, uses ion intermediates to help with inhibition of DNA replication and activation of apoptotic pathways. This is accomplished by phosphoramidate mustard creating DNA crosslinks (interstrand/intrastrand) at the 7-nitrogen atom which initiates cellular death pathways. As a bi-product of the transformation of aldophosphamide into phosphoramidate mustard acrolein is also formed (de Jonge, Huitema, Rodenhuis, & Beijnen, 2005). Like many other metabolites derived through phase II xenobiotic metabolism, acrolein is far more toxic than its derivative cyclophosphamide. Acrolein as an electrophilic α, β -unsaturated aldehyde, is implicated in off-

target effects including bladder hemorrhagic cystitis and cardiotoxicity. Due to its electrophilic nature acrolein is highly capable of reacting rapidly at several cellular sites, coupled with its cellular irritation effects, its presence proves to be a highly problematic and is attributed with being the main source cyclophosphamide treatment toxicity (Kehrer & Biswal, 2000). At low concentrations acrolein inhibits cell proliferation without inducing apoptosis, while at high concentrations its presence may result in secondary apoptosis promotion (Mohammad et al., 2012).

Select chemotherapeutic drugs are associated with several cardiotoxic side effects. Complications transverse a wide spectrum but more common side effects of chemotherapeutic treatment include pericarditis, isolated arrhythmias, myocarditis, cardiomyopathy, and cardiac failure. Risk factors associated with individuals developing cardiotoxicity pose treatment of a chemotherapeutic drug is directly associated with the cumulative dose per treatment. Alkylating agents contradict anthracycline agents which follow a dose-response dependent relationship or lifetime dose. Incidences of disease are highly dependent upon a dose-concentration per administration (Dadfarmay, Berkowitz, & Kim, 2012). High dose concentrations of cyclophosphamide therapy can result in cardiac toxicity. High dose concentrations are defined as 144-270 mg/kg, administration at these level can lead to death which is endorsed by heart failure (Chan, 1984). Doses attributed with a 25% incidence of cardiotoxicity are ~ 240mg/kg, although cardiac toxicity has been seen in dosage as low as 144 mg/kg. Cyclophosphamides clinical manifestations of cardiotoxicity include arrhythmias, cardiac enzymes elevation, congestive heart failure, electrocardiographic voltages dampening, pericarditis and transient cardiomegaly (Langford, 1997). Current data on cardiotoxicity of cyclophosphamide shows a need for developing intervention methods to help mitigate the damages of acrolein induced toxicity. Administration of cyclophosphamide at high treatment levels is associated with acute-cardio-

toxicity. This associated toxicity has shown that GSH plays an integral role in protection against cardio-toxicity, acrolein prompted glutathione depletion is tied to cyclophosphamide associated cardiotoxicity (de Jonge et al., 2005).

H9c2(2-1) Model

A century has passed since Ross Harrison completed the first successful culturing of cells, leading him to be known as the father of cell culture. Although cell culturing techniques began in the 20th century, techniques continue to evolve and advance today (Rodriquez-Hernandez, 2014). The establishment of the H9c2 line in the 1970's has proven that this cell model is useful for utilization in toxicological testing. The H9c2 (2-1) is a myoblast sub-clone derived from embryonic BDIX rat heart tissue the original clonal line developed by B. Brandt and B. Kimes (Hescheler et al., 1991). The H9c2 (2-1) cell line is largely valuable when compared to primary cultures or whole tissues due to its ability to remain more homogenous phenotypically, this stability transcends electrophysiology, morphology and biochemistry properties. These characteristics help make the H9c2 (2-1) cell line an excellent model choice when studying cellular development or cellular death. Studying culturing conditions has shown the H9c2 (2-1) cell line successively propagates for months without undergoing any characteristic changes (Kimes & Brandt, 1976). The H9c2 (2-1) cell line is proven in-vitro model for studying cardiac and skeletal muscle. Additionally it is invaluable model due to its ability to remain a myoblast when serum concentration are supported, providing multiple generations for testing helping to reduce the need for controlling batch variation. The ability to test H9c2 cells within a reasonable propagation range help to ensure treatment is performed on cells similar in terms viability, morphology, and biological properties. The H9c2 (2-1) cell line is also valuable due to its ability to differentiate when serum concentration are reduced allowing the newly differentiated cells to contain several

elements of cardiac cells. These similarities allow differentiated cells to be used for testing cardiovascular diseases, including the assessment of preventative measures and mechanistic pathways (Sardao, Oliveira, Holy, Oliveira, & Wallace, 2007). The in-vitro model for H9c2 cells is currently used to evaluate and manipulate signaling pathways, cellular mechanism, and enzymatic signaling involved in cardiotoxicity. More specifically the use of H9c2 (2-1) cells lines has helped to distinguish drug-induced cardiotoxicity characteristics along with possible intervention methods (Aboutabl & El-Kadi, 2007). In recent studies the H9c2 model has confirmed that cultured primary cardiomyocytes have the ability to be used for studying the hearts metabolic capacity. Stemming from these results the H9c2 cell line was also assessed for its ability to be used as an in-vitro model for heart enzymes associated with drug metabolism. The authors were able to show that expression of CYP1A1 and 1B1 occurs in H9c2 cell lines, additionally the expression can be manipulated through the addition of an inducer (Zordoky & El-Kadi, 2007). Studies have also shown that cellular viability of the H9c2 cell line can be measured by using 3-(4,5-Dimethylthiazol-2-Yl)-2,5-Diphenyltetrazolium Bromide (MTT) levels (Aboutabl & El-Kadi, 2007).

Poly(ADP-Ribose) Polymerase

Current knowledge of enzyme family of Poly(ADP-Ribose) Polymerase (PARPs) has led to the discovery of 18 known members, each varies based on cellular function, molecular weight, composition, location, but all have conservation that is supported by ADP-ribosylating catalytic domain. Poly(ADP-Ribose) polymerase is classified as a chromatin-associated nuclear enzyme, its activation occurs due to DNA damage. DNA repair is an extremely energy-dependent process and apoptosis is an extremely energy-dependent process. As DNA damage is assessed and

repaired, cellular energy will be depleted based on the extent of the damage. An integral part of the process is carried out by the DNA repair enzyme poly(ADP-Ribose) Polymerase. PARP activation occurs when a cell undergoes DNA damage, typically in the form of strand breaks (Jin & El-Deiry, 2005). Through the attachment of poly(ADP-Ribose) units the cell can modify nuclear proteins. Activated PARP leads to poly(ADP-Ribosyl)ation of many cellular proteins (histones, DNA, topoisomerases I & II, PARP) protein activation in turn leads to activation of different pathways (Kaplan, O'Connor, Hake, & Zingarelli, 2005). Poly(ADP-Ribose) polymerase as an enzyme works by detecting DNA strand breakage. After detection of DNA damage PARP catalyzes ADP-ribose transfer from co-enzyme NAD^+ to help bind DNA. (Dantzer et al., 1999) Cellular damage can occur directly through genotoxic agents (oxidation, ionization, alkylation) or as an indirect process post-enzymatic incision. Cellular viability is highly dependent upon the energy depletion as cells undergo repair processes.

PARP-1 which is the most abundant isoform of PARP in the human body is found in the nucleus of the cell, its main function is the detection of single-stranded DNA breaks (SSB). PARP-1 also plays an integral role in cell death, over-activation of PARP-1 leads to significant genomic stress thus causing extreme cellular inflammation due to ATP & NAD depletion (Rouleau, Patel, Hendzel, Kaufmann, & Poirier, 2010). These energy depletions will lead the cell to undergo cellular death through necrosis. Previous studies have confirmed a direct inverse relationship between NAD^+ and PARP. Decrement of NAD^+ affects cellular glycolysis including the Krebs cycle and the redox state of cells (Bouchard, Rouleau, & Poirier, 2003). PARP-1 is also attributed to causing cellular death through apoptosis, this can occur through several processes including caspase-dependent apoptosis, factor-mediated, and caspase-independent apoptosis. Additionally PARP-1 interaction with a down-stream cell death effector (PAR polymer) leads to

parthanatos cell death. PARPs role in all forms of cellular death including programmed, necrosis and apoptosis is dependent upon the amount of PARP activation, pathway selection, cellular metabolic status, and intervention factors (Rosado, Bennici, Novelli, & Pioli, 2013). The difference between apoptosis and necrosis is determined by biochemical and morphological features. Necrosis is defined as the occurrence of cell death as a consequence of acute damage due to disease or injury which lead to an inflammatory response. Apoptosis is characterized as a programmed cell death (Hong, Dawson, & Dawson, 2004). Early phase apoptosis is triggered when transient PARP activation occurs (pre-caspase-mediated-cleavage) and is controlled by the integral relationship between PARP and poly(ADP-ribosyl)ation. PARP as an important determinant of programmed cell death is responsible for inhibiting or selection apoptosis or necrosis pathways. During apoptosis PARP cleavage occurs parallel to caspase activation. PARP cleavage is believed to be responsible for the depletion of energy needed in late-stage apoptosis (Herceg & Wang, 2001). Within apoptosis and necrosis there are well defined cell death processes which are unique to injury induction and cell type. PARP-1 is responsible for PARP-1 mediated apoptosis-inducing factor (AIF). This pathway is linked to ischemic injury and excitotoxic cell death. Hypothesis for PARP-1 mediated cell death involves the rapid depletion of cellular ATP and NAD⁺ due to the over activation of PARP. The reduction of these energy sources affects cellular metabolism and lead to apoptosis. Cell death is heavily dependent upon mitochondria (cellular powerhouse) and nucleus (DNA) health. When either of these organelles is damaged beyond repair signaling determines cellular death pathways, which are dependent upon PARP (Hong et al., 2004).

Clinical trials are evaluating PARP-1 inhibitors' ability to be used as a therapeutic agents, primarily for tertiary care of cancers, inflammatory and autoimmune diseases. The use of an

inhibitor is proving beneficial due the role of PARP in DNA damage detection and base excision repair. PARP inhibitors have been shown through several experimental models to have protective effects against acute and chronic inflammatory diseases (Rosado et al., 2013). In-vitro studies have shown that use of a PARP inhibitor helps render a cell resistant to death by certain inducers, one of which including alkylating agents. These same studies demonstrated that PARP inhibition has shown protective for skeletal muscular and cardiac tissues when ischemia reperfusion was the attributed cause of damage (Herceg & Wang, 2001). PARP inhibitors are chemical agents that are designed to compete at the enzyme activation sites with NAD⁺. When a PARP inhibitor is introduced it acts as a competitive agent against PARP, preventing the repair of DNA damage (Rouleau et al., 2010).

DIQ 1,5-dihydroxyisoquinoline

DIQ 1,5-dihydroxyisoquinoline (C₉H₇NO₂ CAS No. 5154-02-9) is a potent PARP inhibitor that is activated by nitric oxide. Previous studies have shown 1,5-dihydroxyisoquinoline (DIQ) to have a high selectivity for PARP inhibition, pharmacological studies have shown this inhibition helps with the reduction of myocardial damage and increases the viability of cells by inhibiting apoptosis. In-vivo studies of rats which were treated with DIQ showed that PARP-1 inhibition resulted in reduction of infarct size and significant cardio protection, especially in reperfusion linked injury. DIQ has been shown to inhibit PARP –induced inflammatory responses which lead to cells undergoing necrosis (Kaplan et al., 2005). PARP inhibitors have also shown that following a sublethal-treatment of alkylating agents have the ability to suppress certain signaling pathways driving the damaged cell towards apoptosis instead of necrosis. This is further

characterized through PARP cleavage and PARPs inactivation by caspase-3, both of which are proven markers of that the damaged cell has undergone apoptosis (Dantzer et al., 1999).

CHAPTER TWO:

METHODS

Cell Culture

H9c2(2-1) Rat Embryonic Myoblasts cell line were obtained from the American Type Culture Collect (ATCC) (Manassa, VA) and cultured under humidified conditions, with a 5% CO₂ at 37°C. Cellular medium consisted of Debulcco's Modified Essential Medium (DMEM) (Corning, Manassa, VA) containing 1% - 100U/mL and 100mg/mL penicillin and streptomycin, 10% fetal bovine serum (ATCC), and 1% L-glutamine. (Zordoky & El-Kadi, 2007) Every two-three days medium was changed to provide cells with fresh nutrients. Subdivision of cells occurred when plates reached 80-90% confluence to maintain cells exponential growth. Subdivision was performed by aspirating then washing the plates with phosphate buffered saline (PBS) without calcium or magnesium (Corning) followed with a light trypsinization [0.1% Trypsin EDTA in PBS (Corning)] incubated at 37°C for 5 minutes. The trypsinization reaction was stopped through adding a 1:1 of DMEM, cells were then separated through centrifugation at 250 x g for 4 minutes. Post-centrifugation, supernatant was aspirated allowing resuspension of cells with fresh DMEM. Cells were either plated in tissue-culture treated plates for testing or re-plated to continue propagation. The H9c2(2-1) cells used for experimentation fell within the 5th -12th passage to help ensure stability, consistency and reduce the likelihood of genotype-variation. Exposure periods would only occur after allowing cells sufficient time to reattach to plates, time periods were determined by analysis performed.

Treatment

H9c2(2-1) cells were plated into tissue culture-treated microplates at 1,000 cells per well (96-well) or 75,000 cells per well (24-well) 72 hours prior to MTT or PARP activity assessment, respectively. For AST cells were plated at 10,000 cells per well into 96-well plates 48 hours prior to activity assessment. To prepare for biological marker experimentation, cell were aspirated, washed, and underwent a 30 minute pre-incubation with either a vehicle or PARP inhibitor. PARP inhibitor groups received 100 μ M DIQ 30 minutes prior to dosing, and paired with vehicle-only (DMSO) controls. Replacement medium contained either a 0.3% vehicle (DMSO) or 0.3% PARP inhibitor DIQ. Cells were then underwent a 30 minute exposure period with or without the PARP inhibitor DIQ with acrolein at concentrations varying between 10 μ M and 1000 μ M; controls received medium containing hydroquinone at the same dilution as the 1000 μ M acrolein group. For PARP assay experimentation cells were not treated with PARP inhibitor, cells were treated with acrolein only at two time points, 30 or 55 minutes respectively. For MTT and AST cells underwent a 30 minute pre-incubation with either a vehicle or PARP inhibitor, cells were then underwent a 30 minute acrolein exposure followed by a wash out period. MTT and AST test were given a 100 μ M DIQ PARP inhibitor and then groups were treated with acrolein at concentrations varying between 10 μ M and 1000 μ M.

Poly(ADP-Ribose) Polymerase Activity

For PARP activity assessment, cells were treated with acrolein for 30 or 55 minutes, lysed in a PARP stabilizing buffer, and protein quantified via the Bradford method. A 10X stock solution which was diluted down to 1X PARP stabilizing buffer, was iced, and mixed with samples on ice. Each 24-well plate was iced and then received 75 μ l of cold 1X PARP buffer per well. PARP lysis

buffer is made fresh each treatment day by diluting down from a 10X stock PARP buffer solution. The 10X PARP buffer solution consisted of tris base (500 mM), magnesium chloride $MgCl_2 \cdot 6H_2O$ (20 mM), triton x-100 (1% or 0.01), bovine serum albumin (1000 $\mu g/mL$), hydrochloric acid HCl (1.78 M pH to 8.00), and autoclaved U.P. H₂O to bring to final volume. For PARP analysis protein quantification was used to set all samples to the required 8 μg of protein. The Bradford Reagent was prepared using Marion M. Bradford's recipe of dissolving 100 mg of Coomassie Blue into 50 ml of 95% ethanol solution, additionally 100 ml of 85% phosphoric acid solution was added. The final solution was then diluted down into a 1 liter total volume solution. The Bradford Reagent final concentrations are 0.01% Coomassie Blue (w/v), 8.5% phosphoric acid (w/v) and 4.7% ethanol (w/v). (Bradford, 1976). This solution then underwent double filtration before being used for protein quantification of PARP lysis samples. Standards used to build the curve for protein quantification included 2,000 / 1,000 / 500, 250, 125, 65.5, 31.25, 15.625 and 0. These standards were built using the bovine serum albumin (BSA) albumin standard ampules provided in the BCA protein assay kit (Thermo Fisher). Standards and samples were run in duplicates and read via UV-VIS spectrophotometer at 595 nm. Raw data for each duplicate was averaged, blanked and quantified to determine the dilution concentration to standardize all samples to 8 μg protein for loading in the in house PARP assay.

To evaluate Poly(ADP-Ribose) Polymerase activity and in house PARP Assay was used which uses a quantitative colorimetric endpoint. The protocol for this assay spans across a three day period. On the first day a high binding 96-well plate (Fisher -Perkin Eelmer) is prepared to plate histones. A histone plating solution is made and then 50 μL of histone plating solution is added to each well. The histone plating solution consists of 90 mM sodium carbonate Na_2CO_3 , 10 mM sodium bicarbonate $NaHCO_3$, histone solution 0.1 mg/ml and autoclaved U.P. H₂O (to bring

to final volume). After each well receives the plating solution the plate is sealed with parafilm and incubated overnight at 4°C to allow the histones to adhere to the plate. The second day involves blocking the plate. The plate undergoes a series of washes with each wash including a 5 minute incubation period at 23°C. The first wash solution consists of Phosphate Buffered Saline supplemented with 0.05% Tween-20 (PBS-T), 200 µl/well the wash is repeated twice. The second wash solution consists of Phosphate Buffered Saline (PBS), 200 µl/well also repeated twice. Following the final wash a 3% BSA blocking buffer is added to each well followed by an overnight incubation at 4°C. The third day of this assay involves the detection of PARP.

PARP activity was assessed using 8 µg of lysate, based on the results of the Bradford protein quantification. Preparation of samples included dilution in 1X PARP buffer prepared on ice, PARP HAS standards for determining calibration curve are also diluted using 1X PARP buffer prepared on ice. A working PARP cocktail solution is prepared immediately prior to use. This solution is diluted down from a 10X PARP cocktail stored in -20°C into a 1:10 solution using autoclaved U.P. H₂O. The 10X PARP cocktail contains NAD⁺ and Biotinylated-NAD; the sum of both NAD^{+/B} in the 1X working reagent is 3 mM. Immediately prior to use a 1:10 of Sheared Herring Sperm DNA is added into 1X PARP cocktail. Once all cocktails and samples have been prepared the plate is removed from the 4°C refrigerator and undergoes two wash cycles of 200 µL of PBS-T and PBS repeating the wash regime from day 2. Post washing 25 µL of PARP HSA standards and samples were added in duplicates to their respective wells, this is followed by the addition of 25 µL of 1X PARP cocktail. Mixing occurs via tapping followed by a 60 minute incubation at 21°C. Following PARP cocktail incubation plates are washed 3 times consecutively each with PBS-T and PBS. Post washing 50 µL of 1:60,000 Streptavidin-HRP is added, mixed, and then incubated at 21°C for 60 minutes. Following Streptavidin-HRP incubation plates are

washed 3 times consecutively each with PBS-T and PBS. Post washing 50 μ L 3,3',5,5'-Tetramethylbenzidine (TMB) is added in the dark to each well, incubation occurs for 30 minutes at 21°C. Wells will turn bright blue based on PARP activity. Post incubation 65 μ L of 0.2M hydrochloric acid is used to stop the reaction. Plates are mixed and then stand for 10 minutes before being read via UV-VIS spectrophotometer at 412 nm.

Cytotoxicity Assessment

MTT, 3-(4,5-Dimethylthiazol-2-Yl)-2,5-Diphenyltetrazolium Bromide

For MTT activity assessment, cells were plated at 1,000 cells per well (96-well), pre incubated with DMSO or DIQ and then treated with acrolein for 30 minutes. Standards were ran in triplicates, while samples were ran in 6 replicates. Standard curve was built by plating at 2,000/ 1,500/ 1,000/ 800, 600,400,200 and a DMEM blank. Samples were aspirated, washed, and replaced with 50 μ L DMEM containing 0.3% DIQ or 0.3% DMSO for a 30 minute pre-incubation. Post incubation samples were treated with 50 μ L DMEM containing acrolein at concentrations varying between 10 μ M and 1000 μ M; controls received medium containing hydroquinone at the same dilution as the 1000 μ M acrolein group. Following treatment cells were aspirated, washed, and replaced with 50 μ L fresh DMEM followed by a 4 hour wash-out period. Thereafter, cells were incubated for 2 hours with MTT at a 1:10 dilution at standard culturing conditions. MTT-supplemented medium was then replaced with 100 μ L DMSO in order to solubilize the reduced formazan in preparation for UV-VIS measurement at 570 nm. For analysis standards were blanked against DMEM, samples were blanked against DMEM containing 0.3% hydroquinone solution.

AST, Aspartate Aminotransferase

For AST cells were plated at 10,000 cells per well (96-well). Samples were run in triplicates, they were aspirated, washed, and replaced with 50 μ L DMEM containing 0.3% DIQ or 0.3% DMSO for a 30 minute pre-incubation. Post incubation samples were treated with 50 μ L DMEM containing acrolein at concentrations varying between 10 μ M and 1000 μ M; controls received medium containing hydroquinone at the same dilution as the 1000 μ M acrolein group. Following treatment cells were aspirated, washed, and replaced with 35 μ L fresh DMEM followed by a 6 hour wash-out period. Thereafter, 10 μ L medium of sample was re-plated in duplicates into a new 96-well plate. Each well plate contained standards, blanks, and AST calibrator also plated at 10 μ L in duplicates. The standard curve was derived using Oxaloacetate diluted in PBS to 10 μ M then serially diluted to 5 μ M, 2.5mM 1 μ M, 0.5 μ M, 0.25 μ M, 0.125 μ M. Once all standards, samples, blanks and calibrator were plated 50 μ L AST Substrate was added every 10 seconds using a multichannel pipette. Plates were then incubated for 10 minutes at 37°C. Following substrate incubation 50 μ L AST color developer was added every 10 seconds using a multichannel pipette. Plates were again incubated for 10 minutes at 37°C. Finally 100 μ L 0.2M HCL was added using a multichannel pipette. Plates were then incubated for 10 minutes at 21°C. Thereafter, samples were ran in UV-VIS measurement at 530 nm. For analysis standards were blanked against PBS while samples were blanked against DMEM. Quantified results were converted using 78.8 IU/L to standardize AST signal.

Spectrophotometric Quantification

Assays which required assessment of colorimetric endpoints (AST, MTT, and PARP) were quantified using the μ Quant Spectrophotometer (BioTek, Winooski, VT) coupled with the KC-

Junior Analytical software (BioTek). Each colorimetric endpoint that was assessed was set at the wavelength suggested by the manufacturer. Assays were read via UV-VIS spectrophotometer at: PARP 412 nm, MTT 570 nm, and AST 530 nm.

Statistical Analysis

Statistical analysis was performed utilizing Microsoft Excel. Standards were averaged, blanked and quantified to be used for analyzing samples. Samples were averaged, blanked, and used standards quadratic equation to be quantified. Additional analysis was performed to derive fold and standard deviation values. Fold averages and fold deviations were further analyzed by aggregating all of the test to determine each treatment group's average, standard deviation, 95% confidence interval and t-test. Aggregated data was processed using SPSS predictive analytics software to identify and eliminate outliers. Outliers were classified as falling 3 standard deviations below/above the standard mean. Statistical significance was determined when the probability of reaching the measured statistic fell at or below 5.0 % ($p \leq 0.05$).

CHAPTER THREE:

RESULTS

Summary: Cytotoxicity

Looking at the H9c2 (2-1) cell line as an in-vitro model is beneficial for analyzing the role that Poly(ADP-Ribose) Polymerase and PARP inhibitors play in acrolein induced-cytotoxicity. In assessing poly(ADP-ribose) polymerase activity post treatment across two time points it was apparent that a treatment-dependent relationship was demonstrated when assessing PARP activity against acrolein concentration. For this analysis two bio-markers of cytotoxicity were utilized to interpret the degree of cellular death post treatment. First cellular viability was assed using the mitochondrial succinate dehydrogenase-dependent MTT reduction assay. Then aspartate aminotransferase (AST) assay was used to measure colorimetric analysis in units/liter (U/L) the reaction between each lysates' enzyme and substrate. Aspartate aminotransferase was able to provide evidence of membrane degradation, cellular damage and ultimately viability offering a comparison between treatment and vehicle medium. While signal strength was week and fell below detection limits in lower treatment groups the AST assay still represented a relevant toxic endpoint. Both of these assays demonstrated DIQ's ability to increase cellular viability, although statistical significance was only reached in two treatment groups.

Poly(ADP-Ribose) Polymerase Activity

To prepare for PARP analysis 75,000 cells were plated into 24-well plate to allow for a 30 minute or 55 minute time exposure to acrolein treatment groups varying in concentrations of 10

μM -1000 μM . Post exposure, cells were washed using PBS and lysed using a prepared ice-cold lysis buffer which was supplemented with Triton-X-100. Lysis of cells occurred over ice and protein lysates were collected in triplicates, with one being used for quantification via Bradford method. For the PARP assay the amount of purified cellular protein required was standardized to 8 micrograms per sample. The standard curve was calibrated and quantified for further analysis of PARP activity in samples. Samples duplicates were first averaged, blanked and then quantified against the quadratic equation generated by the standards. This created an x-axis of PARP activity in 8 μg against the y-axis of treatment groups. The lowest effective concentration of toxicity at 30 minute exposure was found at 25 μM (PARP Activity 1.65-fold control) [Figure 1.] which returned to baseline at 100 μM ; concentrations at or above 250 μM results in significant PARP activity reductions (≤ 0.46 -fold control). This evidence suggests that acrolein induced cardiotoxicity may be modulated through PARP inhibition. . There was no lowest effective concentration of toxicity at 55 minute exposure. [Figure 2.] All concentrations when compared to control results had significant PARP activity reductions (≤ 0.98 -fold control). This evidence suggests that acrolein induced cardiotoxicity may be modulated through PARP inhibition, but against longer exposure periods samples folds will significantly reduce linearly with time. [Figure 3.]

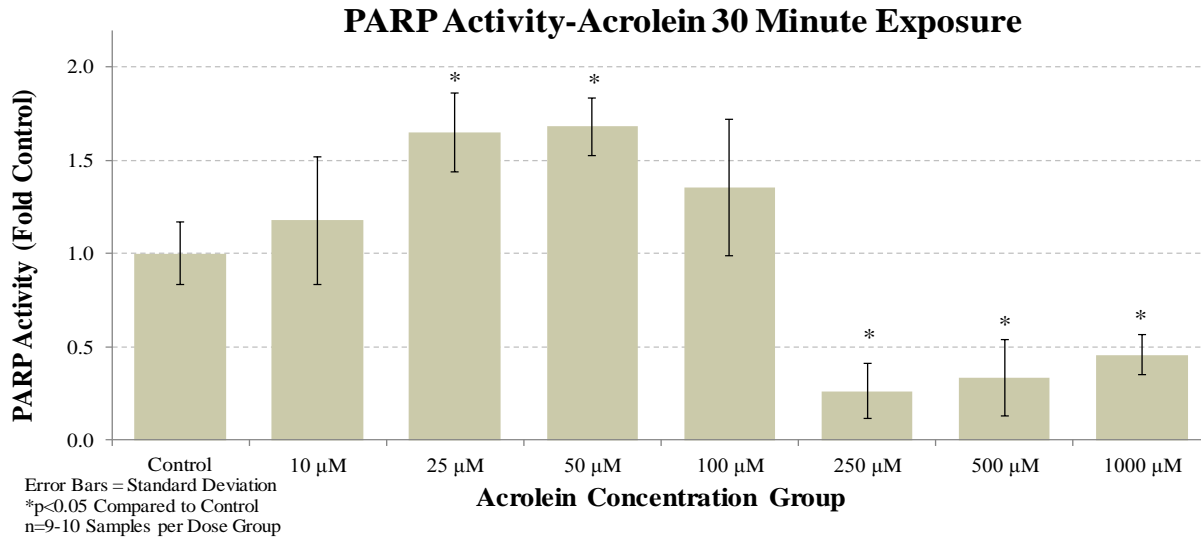


Figure 1: Poly(ADP-Ribose) Activity 30 Minutes: PARP Activity (fold-control) assessed 30 minutes after exposure with acrolein. Two positive statistical significant differences were observed when compared to control in the 25 μM & 50 μM treatment groups. All treatment groups ≥250 μM reached negative statistical significance when compared to fold control.

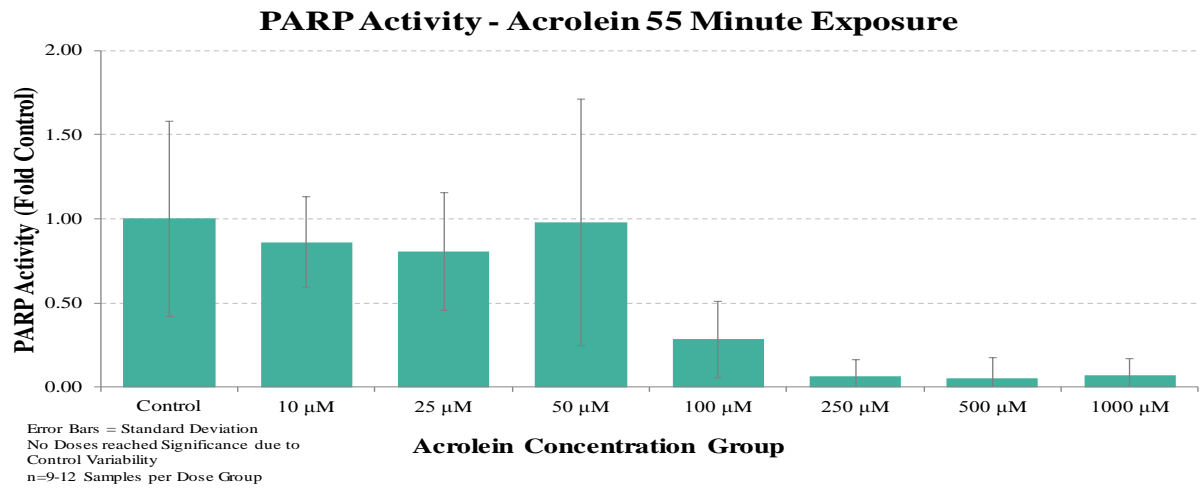


Figure 2: Poly(ADP-Ribose) Activity 55 Minutes: PARP Activity (fold-control) assessed 55 minutes after exposure with acrolein. No treatment groups reached statistical significant All treatment groups ≥10 μM had PARP activity that fell below fold control.

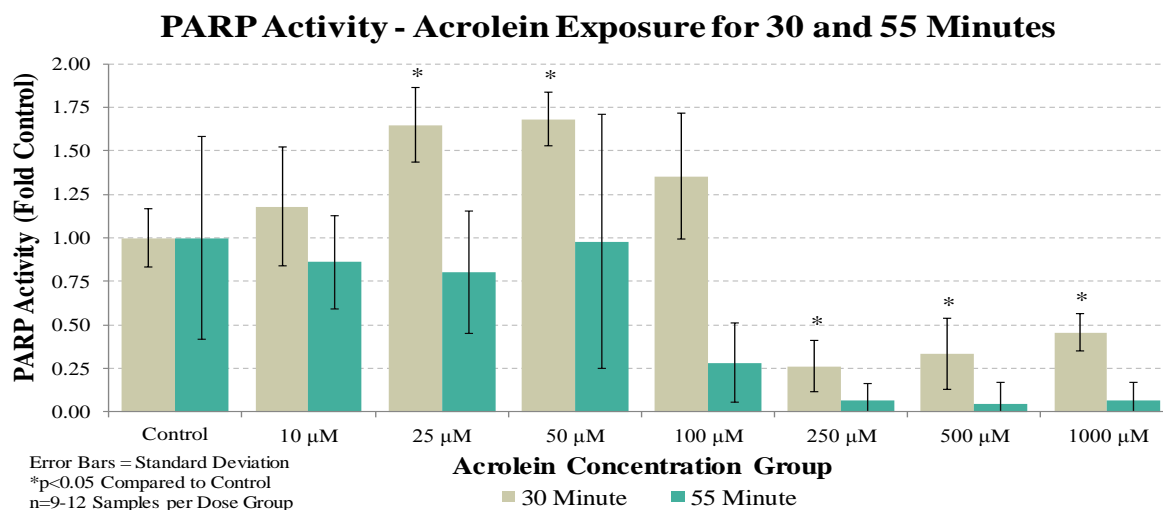


Figure 3: Poly(ADP-Ribose) Activity Comparison: PARP Activity (fold-control) assessed at 30 & 55 minutes after exposure with acrolein. Only treatment groups at the 30 minute time point reached positive/negative statistical significance. At either time point acrolein treatment groups $\geq 250 \mu\text{M}$ had PARP activity that fell below fold control.

Toxicological Endpoints

MTT, 3-(4,5-Dimethylthiazol-2-Yl)-2,5-Diphenyltetrazolium Bromide

To prepare for MTT analysis 1,000 cells were plated into 96-well plate to allow for a 30 minute time exposure to acrolein treatment groups varying in concentrations of 10 μM -1000 μM . Post exposure, cells were washed using PBS, underwent a 4 hour wash out, and then had medium replaced with 1:10 dilution of formazin for a 2 hour incubation. Cells were then aspirated and formazin crystals were re- solubilized using DMSO. The MTT analysis was preformed through a colorimetric assay which was used to determine the amount of cellular enzyme activity present based on the amount tetrazolium dye reduced. The reduction produces an insoluble formazan which is re-solubilized to produce a purple color. Based on the color gradient read via UV-VIS spectrophotometer cytotoxicity can be assessed (Riss et al., 2004). Standard curves were built using cell plating ranging from 200-2,000 cells, readings were calibrated then quantified for further analysis of MTT activity in samples. Treatment groups duplicates were averaged, blanked and then quantified against the standards. In MTT the concentrations of toxicity for acrolein which the

DIQ treatment had the greatest protection was found at 25 μM & 50 μM when comparing to the vehicle in the MTT analysis. (MTT Activity 0.05 & 0.003 T-Test) [Figure 4.] At ≥ 250 μM DIQ provided no significant protections (MTT Activity 0.119, 0.527, 0.463 T-Test). At ≤ 100 μM DIQ protection was limited (MTT Activity 0.065 T-Test). Statistical analysis was further assessed to determine if any outliers were skewing data results. Treatment groups' data were assessed by either vehicle or DIQ. In vehicle treatment groups (DMSO) two outliers were assessed. [Figure 5.] After their removal standard deviations in the 100 μM & 1000 μM reduced. (100 μM 0.37 \rightarrow 0.21 & 1000 μM 0.05 \rightarrow 0.03) In PARP inhibitor treatment groups (DIQ) two outliers were assessed. [Figure 6.] After their removal standard deviations in the 25 μM & 50 μM decreased. (25 μM 0.28 \rightarrow 0.16 & 50 μM 0.25 \rightarrow 0.12)

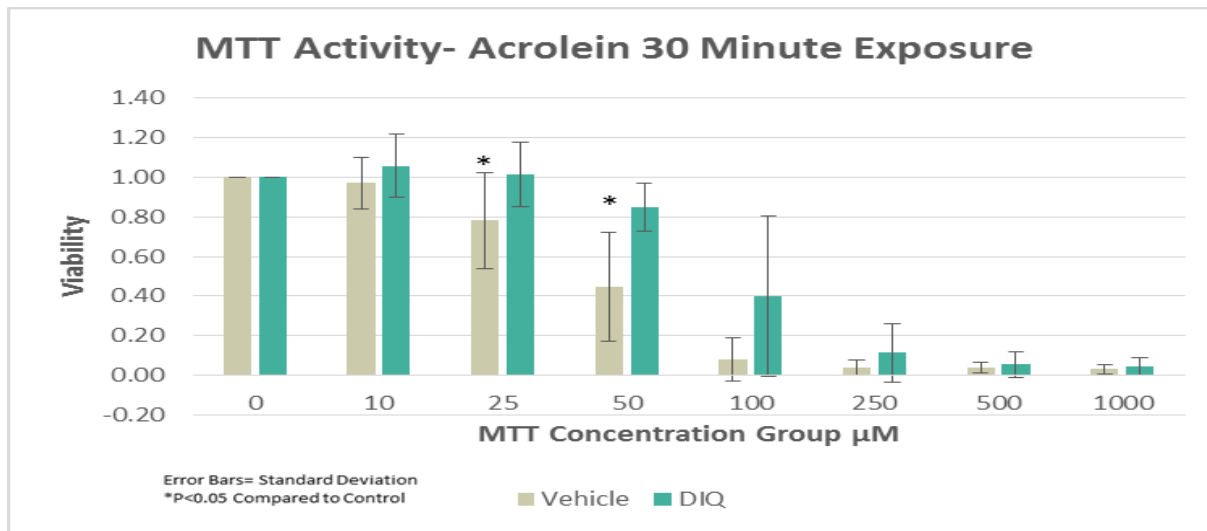


Figure 4: MTT Activity: MTT Activity (fold-control) assessed 30 minutes after exposure with acrolein. Two positive statistically significant differences were observed when compared to control in the 25 μM & 50 μM treatment groups. All treatment groups ≥ 250 μM showed some protections but none reached statistical significance when compared to fold control. At ≤ 100 μM DIQ protection was limited

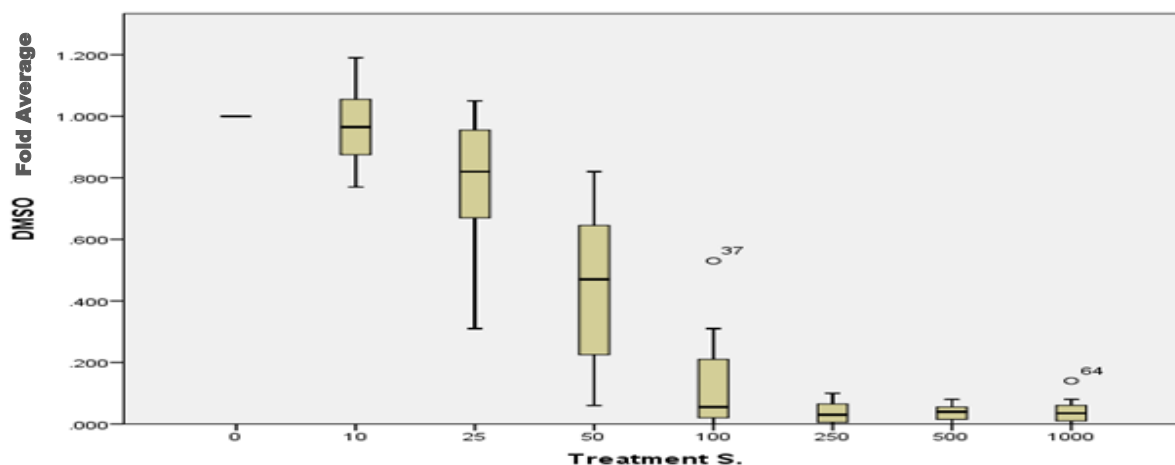


Figure 5: Vehicle Box Plot MTT: Outliers were processed using SPSS predictive analytics software. Circles noted in reader results denote outliers. Outliers were processed using aggregated fold averages for all trials. °37 Fell under Trial 5 -100 μ M treatment group. The fold value .53 fell more than 3 standard deviations above the average after its removal from the data set so its value was thrown out. °64 Fell under Trial 8 -1000 μ M treatment group. The fold value .14 fell more than 3 standard deviations above the average after its removal from the data set so its value was thrown out.

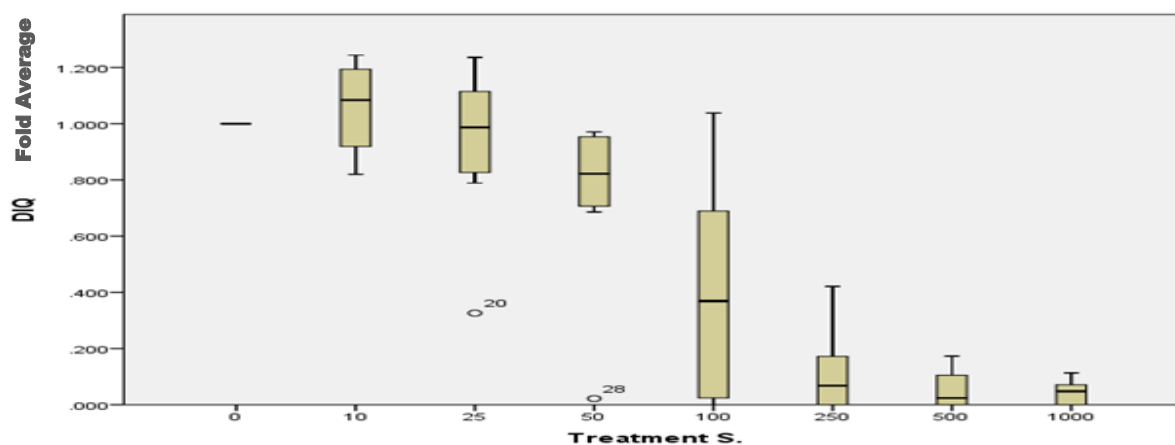


Figure 6: DIQ Box Plot MTT: Outliers were processed using SPSS predictive analytics software. Circles noted in reader results denote outliers. Outliers were processed using aggregated fold averages for all trials. °20 Fell under Trial 4 -25 μ M treatment group. The fold value .33 fell more than 3 standard deviations below the average after its removal from the data set so its value was thrown out. °28 Fell under Trial 4 -50 μ M treatment group. The fold value .22 fell more than 3 standard deviations below the average after its removal from the data set so its value was thrown out.

AST, Aspartate Aminotransferase

To prepare for AST analysis 10,000 cells were plated into 96-well plate treated at groups varying in concentrations of 10 μ M-1000 μ M for a 30 minute exposure period. Post exposure, cells were washed using PBS, underwent a 6 hour wash out with fresh medium, and then had 10 μ l of lysate medium collected and replated in duplicate into a new 96-well plate. In this assay glutamate

oxaloacetate transaminase (GOT) is reduced using tetrazolium enzymatic reaction with oxalacetic acid yielding a red compound to be read and standardized against a calibrator. Standard curves were built using Oxaloacetate ranging from 10 μM -0.125 μM . Samples underwent substrate, color developer, and HCL incubations prior to being read via UV-VIS spectrophotometer. For AST the only treatment groups which were read above the detection limits were $\geq 250 \mu\text{M}$. No AST treatment concentrations reached Significance due to control Variability, at 250 μM & 500 μM DIQ protection was limited (AST Activity 0.09 & 0.26 T-Test). In 1000 μM DIQ treatment groups an adverse effect was seen in vehicle treatment groups having higher viability. (AST Activity 0.175 t-test) [Figure 7.] Further statistical analysis was performed using SPSS to determine if any outliers existed for trials. Data was aggregated by either vehicle or DIQ. Statistical analysis was further assessed to determine if any outliers were skewing data results. Treatment groups' data were assessed by either vehicle or DIQ. In vehicle treatment groups (DMSO) no outliers were present. [Figure 8.] In PARP inhibitor treatment groups (DIQ) no outliers were present. [Figure 9.]

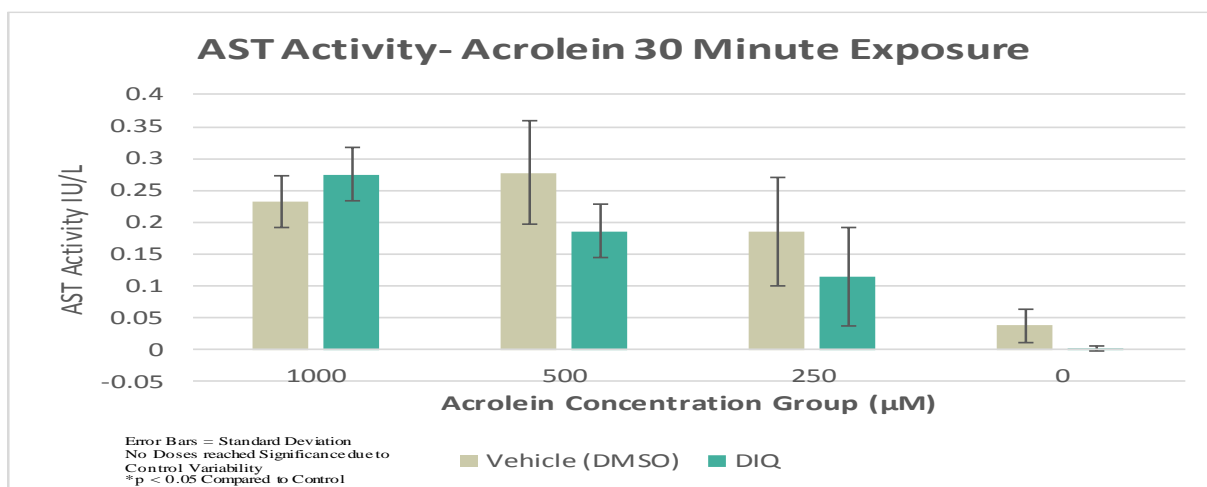


Figure 7: Aspartate Aminotransferase Activity AST Activity (fold-control) assessed 30 minutes after exposure with acrolein. No treatment groups reached statistical significance due to control variability.

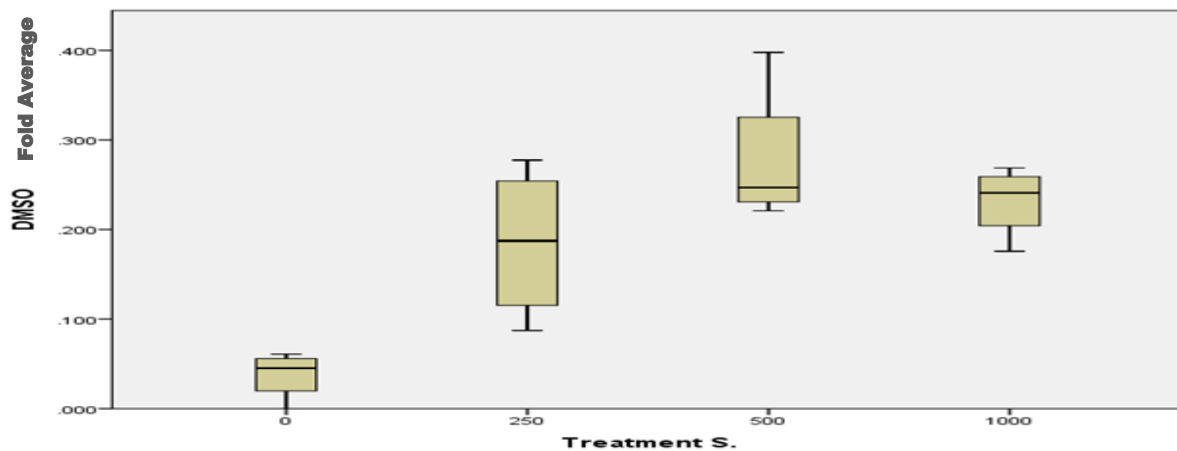


Figure 8: Vehicle Box Plot AST: Outliers were processed using SPSS predictive analytics software. Circles noted in reader results denote outliers. No outliers were detected.

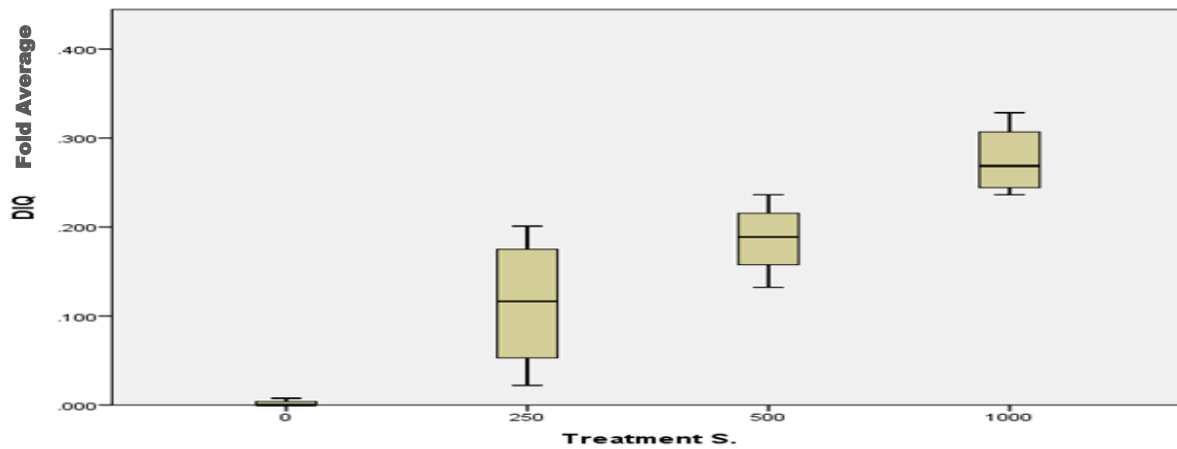


Figure 9: DIQ Box Plot AST: Outliers were processed using SPSS predictive analytics software. Circles noted in reader results denote outliers. No outliers were detected.

CHAPTER FOUR:

DISCUSSION

This investigation explored the role of Acrolein-induced Toxicity using the H9c2 model, and what role PARP inhibitors play in helping reduce cytotoxicity. Chemotherapy induced cardiotoxicity is a well-documented side effect of undergoing prodrug treatments. Cardiotoxicity due to molecular mechanisms of oxidative stress can lead to apoptosis due to cytotoxicity (Angsutararux, Luanpitpong, & Issaragrisil, 2015). Cytotoxic potentials of cyclophosphamide and acrolein are being assessed at in-vivo and in-vitro levels. Understanding the mechanistic differences between administrations of toxicants of cellular vs. whole systems is important for furthering research into preventative measures. Cyclophosphamides toxicity is greatest after it has undergone microsomal oxidation generating acrolein, the cytotoxic aldehyde (Sladek, 1973). Cyclophosphamide activation forms 4-hydroxycyclophosphamide, which is readily diffused within cells and is not a cytotoxic compound. It does spontaneously decompose due to being incredibly instable leading to the formation of phosphoramidate mustard and acrolein. Acrolein is highly reactive aldehyde, making it extremely cytotoxic. Previous studies have contributed ATP reduction as a major contributor to acrolein-mediated necrosis. Possible explanations for the depletion of ATP include the over-activation of PARP, thus leading to reduced ATP because of the energy taking process of PARP's substrate regeneration (Kern & Kehrer, 2002). Another possibility for the enhanced cytotoxicity of acrolein is glutathione depletion at the cellular level due to conjugation (de Jonge et al., 2005). Previous studies have supported that mitochondria lack glutathione biosynthesis enzymes, thus GSH must be transported from the cytosol into the mitochondria by using a high

affinity transporter. This means that acrolein conjugation leads to the depletion of glutathione not GSH oxidation (Arumugam, Thanislass, Rangunath, Niranjali Devaraj, & Devaraj, 1999). Previous studies have also linked the unsaturated nature of acrolein as the cause for the stark depletion of cytosolic glutathione, in-vivo rat studies have shown an unchanged content of GSSG in acrolein-treated rats, and thus GSH oxidation pathways went unused (Arumugam et al., 1999). Potential biomarkers have been identified and could be used to assess the amount of acrolein conjugation occurring in individuals' undergoing chemotherapy treatments of cyclophosphamide. Conjugation of glutathione with acrolein produces 3-hydroxypropylmercapturic acid. Previous studies have found that 3-hydroxypropylmercapturic acid is detectable through urinalysis of individuals and rats treated with cyclophosphamide (Faroon et al., 2008). The ability of 3-hydroxypropylmercapturic acid production as a measurement tool for elucidating the amount of acrolein bi-product produced from chemotherapy treatments should be further assessed.

PARP-1 activation is responsible for mediation of cell death, through signaling downstream apoptotic effectors. PARP-1 activation has been proven to mediate pathways for cells which underwent damage induced through reperfusion injury, reactive oxygen species injury, inflammatory injury, and ischemia injury (Yu et al., 2002). PARP inhibitors are undergoing clinical development to be used as a therapeutic agent. Currently a two-pronged approach is being utilized. First is the targeting of cells that have a genetic predisposition toward death when PARP activity is inhibited. The second therapeutic approach is looking at the benefits of PARP-inhibition to prevent DNA repair, thus forcing cellular suicide (Rouleau et al., 2010). Several studies are actually looking into the second approach to see if PARP inhibitors can be utilized as therapeutic agents for single-agent or combination therapy as anticancer treatment. PARP inhibitors would work as therapeutic agents due to their capacity to block poly(ADP-Ribose) enzymes, these

enzymes help repair DNA damage. PARP inhibition assists with tumor growth limitation, and inhibition of angiogenesis (Rosado et al., 2013). More recently PARP inhibitors have undergone clinical trials to assess their use against BRCA-defective cancer cells. PARP's interaction with BRCA1 and BRCA2 proteins is crucial, if its excision repair was inhibited these types of cancer cells would be unable to repair DNA, thus leading to tumor death (Rosado et al., 2013). As trials continue to progress the medical applications for PARP inhibitors will broaden. While it is apparent that PARP plays an integral role in DNA-mediated cellular death, what role it plays is highly dependent upon the inducer of damage. The paradox is highly perplexing, in some instances of DNA damage typically lower scaled PARP plays a protective role in staving off cell death. In other instances when extensive DNA damage occurs PARP promotes cellular death. PARP's ability to undertake dual-function roles is highly dependent upon cell type, DNA damage extent, cascade activation, and cellular target. PARP as a consumer of energy (ATP / NAD) and nature as a DNA binding molecule are highly dependent: balance of which determines cellular survival (Herceg & Wang, 2001).

Cardio toxicity of alkylating agents like cyclophosphamide are tied directly to the administrated treatment amount of a single dose vs. a lifetime dose response effect (Kumar, Dhankhar, Kar, Shrivastava, & Shrivastava, 2011). Much like previous studies acrolein exposure for this study was assessed with a consistent cell density. This is due to other assessments proving acrolein-induced toxicity was highly dependent upon dose received by each cell verses the treatment concentrated administered to each well. Additionally fold controls were used to assess a base line to establish cytotoxicity in treatment groups (Kern & Kehrer, 2002). The range of treatment groups for acrolein were too high to be considered clinically relevant, but were good for assessing acute high-dose exposure at the cellular level. In terms of PARP analysis no inhibitor

intervention was applied, only time points of acrolein exposure were assessed. Poly (ADP-ribose) synthesis can only occur through members of the PARP family, primarily by PARP-1. When DNA damage is present poly(ADP-Ribosyl)ation levels will be high, absent of DNA damage the levels will be very low (Bouchard et al., 2003). Analysis performed on PARP activity were used to help determine the extent of damage done through the treatment of acrolein. PARP activity increased as acrolein-treatment concentration increased to a point due to greater damage undertaken by the cells. In higher acrolein-treatment groups activity dropped off, most likely due to inhibition of PARP to activation apoptotic pathways. Further analysis of acrolein exposure time-points could give a broader understanding to the activation of PARP due to cytotoxicity. Based on this analysis a trend was revealed that implied PARP activity would linearly decrease across all dose groups as acrolein exposure periods increased. Most likely this would be due to increased damages caused by the prolonged exposure periods.

In terms of cytotoxic assessment this investigation had a few suggestions to offer for future assessment. For MTT analysis this investigation believes that a tighter standard deviation could be achieved through increasing the replication of trials. Additionally one analysis was discarded due to use of a pre-aliquoted DIQ being utilized. This aliquot had been stored at -20°C, its use showed no differences between vehicle and controls in any treatment groups. Further testing was performed using fresh 1,5-dihydroxyisoquinoline, each sequential analysis performed showed a protective factor. Thus it is recommended to prepare fresh PARP inhibitor prior to each trial as pre-aliquoted freezer storage impacted the ability for DIQ to reduce cytotoxic effects. When analyzing the AST assay this investigation proved the importance of insuring high protein in samples run for analysis. Poor performance in AST assays particularly from a poor signal strength can be attributed to loading with low protein (Huang et al., 2006). For future analysis it is

recommended to increase the protein load by increasing the cellular density and decreasing the replacement medium for which to collect the AST lysate. This investigation used a 96-well treated plate, increasing to a 48-well or 24-well with a plating density of 50,000-75,000 cells per well should help all treatment groups to be read above detection. When initially running AST analysis, a 24-hour wash out period was utilized, this resulted in a flat-line for AST signals, resulting in all treatment groups to fall below the detection limit. Two trial runs were performed to determine time points and lysate medium volumes. Time points assessed were 2-hour, 4-hour, 6-hour, 8-hour respectively. A linear relationship was established with AST activity increasing until the 6-hour peak mark, with activity levels severely reduced at 8-hour reading. Additionally analysis was performed to determine the medium volume which would help concentrate AST the best, 35 μ l was determined to be the best volume which would allow for adequate coverage of plate wells thus not skewing results by having cell death attributed to hypoxia vs. treatment. Further analysis should be performed and investigate the levels of caspase-3 as it is a key marker for apoptosis. Cellular fate post-exposure to an alkylating agent is determined through the metabolic state of the cell. Inactivation of PARP by caspase-mediated cleave is responsible for initializing apoptosis having helped block the pathway of necrosis cell death (Jin & El-Deiry, 2005). Since caspase-3 is responsible for the cleavage of poly(ADP-Ribose) polymerase (PARP) during apoptosis, comparative measures of PARP, cleaved PARP, and caspase-3 activity could give a more in-depth analysis to the level of acrolein-induced cytotoxicity. Cleaved PARP is induces apoptosis through chromatin condensation, membrane blebbing and DNA-fragmentation. (Cohen, 1997) Western-blot analysis was performed using Caspase-3 and PARP antibodies to determine MW present in samples. Positive identification of PARP, Cleaved-PARP and Caspase-3 occurred. Digital

imaging of nitrocellulose membranes proved inadequate resolution for inclusion in this report. Use of more advanced imaging techniques in the future could produce a higher quality resolution.

CHAPTER FIVE:

CONCLUSION

This investigation assessed the role of the enzyme poly (ADP-ribose) polymerase (PARP) and PARP inhibitors in acrolein induced toxicity using the established toxicological H9c2 (2-1) cardiomyoblast in-vitro model. Through this analysis the characterization of PARP's role in cytotoxicity was able to be determined. In low concentration PARP activation is suggestive of electrophilic damage of DNA. The inactivation of PARP at higher concentrations imitates apoptotic mediation through activation of caspase-3. Further analysis is needed to investigate PARP cleavage as a marker for apoptosis. Cytotoxic assessment showed that pre-incubation with a PARP inhibitor had a positive trend in increasing cellular viability in all treatment groups, statistically significant protection was reached in 25 μ M & 50 μ M treatment groups. MTT activity showed a positive trend across all treatment groups for increasing when DIQ groups were compared to vehicle groups. AST activity in isolated cell lysates for many lower treatment groups were unable produce a strong enough signal for data characterization of DIQ's protective qualities due samples falling below detection limits. Higher treatment groups which were read above detection showed a positive trend when compared to vehicle groups, but statistical significance was unreached. Further analysis is needed to investigate methodological changes which could lead to an increase in signal strength for AST detection. Further analysis is also needed to investigate more clinically relevant levels of acrolein against longer exposure periods. Testing using the H9c2 cardiomyocyte cell line represents an appropriate model for characterizing the role of PARP in acrolein-mediated cytotoxicity.

REFERENCES

- Aboutabl, M. E., & El-Kadi, A. O. (2007). Constitutive expression and inducibility of CYP1A1 in the H9c2 rat cardiomyoblast cells. *Toxicol In Vitro*, *21*(8), 1686-1691.
doi:10.1016/j.tiv.2007.07.002
- American Cancer Society. (2016). Breast Cancer. Retrieved from
<http://www.cancer.org/cancer/breastcancer/detailedguide/breast-cancer-key-statistics>
- Angsutararux, P., Luanpitpong, S., & Issaragrisil, S. (2015). Chemotherapy-Induced Cardiotoxicity: Overview of the Roles of Oxidative Stress. *Oxid Med Cell Longev*, *2015*.
- Arumugam, N., Thanislass, J., Rangunath, K., Niranjali Devaraj, S., & Devaraj, H. (1999). Acrolein-induced toxicity--defective mitochondrial function as a possible mechanism. *Arch Environ Contam Toxicol*, *36*(4), 373-376.
- Bouchard, V. J., Rouleau, M., & Poirier, G. G. (2003). PARP-1, a determinant of cell survival in response to DNA damage. *Exp Hematol*, *31*(6), 446-454.
- Bradford, M. M. (1976). A rapid and sensitive method for the quantitation of microgram quantities of protein utilizing the principle of protein-dye binding. *Anal Biochem*, *72*, 248-254.
- Chan, M. K. (1984). Cyclophosphamide: a drug profile. *J Assoc Pediatr Oncol Nurses*, *1*(3), 30-33.
- Cohen, G. M. (1997). Caspases: the executioners of apoptosis. *Biochem J*, *326* (Pt 1), 1-16.

- Conklin, D. J., Haberzettl, P., Jagatheesan, G., Baba, S., Merchant, M. L., Prough, R. A., . . . Bhatnagar, A. (2015). Glutathione S-transferase P protects against cyclophosphamide-induced cardiotoxicity in mice. *Toxicol Appl Pharmacol*, 285(2), 136-148.
doi:10.1016/j.taap.2015.03.029
- Dadfarmay, S., Berkowitz, R., & Kim, B. (2012). Irreversible end-stage cardiomyopathy following a single dose of cyclophosphamide. *Congest Heart Fail*, 18(4), 234-237.
doi:10.1111/j.1751-7133.2011.00279.x
- Dantzer, F., Schreiber, V., Niedergang, C., Trucco, C., Flatter, E., De La Rubia, G., . . . de Murcia, G. (1999). Involvement of poly(ADP-ribose) polymerase in base excision repair. *Biochimie*, 81(1-2), 69-75.
- de Jonge, M. E., Huitema, A. D., Rodenhuis, S., & Beijnen, J. H. (2005). Clinical pharmacokinetics of cyclophosphamide. *Clin Pharmacokinet*, 44(11), 1135-1164.
doi:10.2165/00003088-200544110-00003
- Faroon, O., Roney, N., Taylor, J., Ashizawa, A., Lumpkin, M., & Plewak, D. (2008). Acrolein health effects. *Toxicology and industrial health*, 24(7), 447-490.
- Herceg, Z., & Wang, Z. Q. (2001). Functions of poly(ADP-ribose) polymerase (PARP) in DNA repair, genomic integrity and cell death. *Mutat Res*, 477(1-2), 97-110.
- Hescheler, J., Meyer, R., Plant, S., Krautwurst, D., Rosenthal, W., & Schultz, G. (1991). Morphological, biochemical, and electrophysiological characterization of a clonal cell (H9c2) line from rat heart. *Circ Res*, 69(6), 1476-1486.
- Hong, S. J., Dawson, T. M., & Dawson, V. L. (2004). Nuclear and mitochondrial conversations in cell death: PARP-1 and AIF signaling. *Trends Pharmacol Sci*, 25(5), 259-264.
doi:10.1016/j.tips.2004.03.005

- Huang, X.-J., Choi, Y.-K., Im, H.-S., Yarimaga, O., Yoon, E., & Kim, H.-S. (2006). Aspartate aminotransferase (AST/GOT) and alanine aminotransferase (ALT/GPT) detection techniques. *Sensors*, 6(7), 756-782.
- Jin, Z., & El-Deiry, W. S. (2005). Overview of cell death signaling pathways. *Cancer Biol Ther*, 4(2), 139-163.
- Kaplan, J., O'Connor, M., Hake, P. W., & Zingarelli, B. (2005). Inhibitors of poly (ADP-ribose) polymerase ameliorate myocardial reperfusion injury by modulation of activator protein-1 and neutrophil infiltration. *Shock*, 23(3), 233-238.
- Kehrer, J. P., & Biswal, S. S. (2000). The molecular effects of acrolein. *Toxicol Sci*, 57(1), 6-15.
- Kern, J. C., & Kehrer, J. P. (2002). Acrolein-induced cell death: a caspase-influenced decision between apoptosis and oncosis/necrosis. *Chem Biol Interact*, 139(1), 79-95.
- Kimes, B. W., & Brandt, B. L. (1976). Properties of a clonal muscle cell line from rat heart. *Exp Cell Res*, 98(2), 367-381.
- Kumar, S., Dhankhar, N., Kar, V., Shrivastava, M., & Shrivastava, S. (2011). Myocardial injury provoked by cyclophosphamide, protective aspect of hesperidin in rats. *Int J Res Pharm Biomed Sci*, 2(3), 1288-1296.
- Langford, C. (1997). Complications of cyclophosphamide therapy. *European archives of oto-rhino-laryngology*, 254(2), 65-72.
- Mohammad, M. K., Avila, D., Zhang, J., Barve, S., Arteel, G., McClain, C., & Joshi-Barve, S. (2012). Acrolein cytotoxicity in hepatocytes involves endoplasmic reticulum stress, mitochondrial dysfunction and oxidative stress. *Toxicol Appl Pharmacol*, 265(1), 73-82.
doi:10.1016/j.taap.2012.09.021

- Riss, T. L., Moravec, R., Niles, A., Benink, H., Worzella, T., & Minor, L. (2004). Cell viability assays.
- Rodriguez-Hernandez, C. O., Muro, A. L. , Gonzalez, F. J. , Guerrero-Barrera, A. L. . (2014). Cell Culture: History, Development and Prospects. *International Journal of Current Research and Academic Review*, 2(12), 188-200. Retrieved from https://www.researchgate.net/publication/269932638_Cell_culture_History_Development_and_Prospects
- Rosado, M. M., Bennici, E., Novelli, F., & Pioli, C. (2013). Beyond DNA repair, the immunological role of PARP-1 and its siblings. *Immunology*, 139(4), 428-437. doi:10.1111/imm.12099
- Rouleau, M., Patel, A., Hendzel, M. J., Kaufmann, S. H., & Poirier, G. G. (2010). PARP inhibition: PARP1 and beyond. *Nat Rev Cancer*, 10(4), 293-301. doi:10.1038/nrc2812
- Sardao, V. A., Oliveira, P. J., Holy, J., Oliveira, C. R., & Wallace, K. B. (2007). Vital imaging of H9c2 myoblasts exposed to tert-butylhydroperoxide--characterization of morphological features of cell death. *BMC Cell Biol*, 8, 11. doi:10.1186/1471-2121-8-11
- Sladek, N. E. (1973). Bioassay and relative cytotoxic potency of cyclophosphamide metabolites generated in vitro and in vivo. *Cancer Res*, 33(6), 1150-1158.
- Yu, S. W., Wang, H., Poitras, M. F., Coombs, C., Bowers, W. J., Federoff, H. J., . . . Dawson, V. L. (2002). Mediation of poly(ADP-ribose) polymerase-1-dependent cell death by apoptosis-inducing factor. *Science*, 297(5579), 259-263. doi:10.1126/science.1072221
- Zordoky, B. N., & El-Kadi, A. O. (2007). H9c2 cell line is a valuable in vitro model to study the drug metabolizing enzymes in the heart. *J Pharmacol Toxicol Methods*, 56(3), 317-322. doi:10.1016/j.vascn.2007.06.001